J. Phys. B: At. Mol. Opt. Phys. **31** (1998) L393–L400. Printed in the UK PII: S0953-4075(98)90330-3

LETTER TO THE EDITOR

Elastic electron scattering by laser-excited ^{138}Ba$(\ldots 6s6p\ ^1P_1)$ atoms

S Trajmar†‡, I Kanik†§, M A Khakoo§, L R LeClair†+, I Bray‖, D Fursa‖ and G Csanak¶

† California Institute of Technology, Jet Propulsion Laboratory, Pasadena, CA 91109, USA
‡ California Institute of Technology, Division of Chemistry and Chemical Engineering, Pasadena, CA 91109, USA
§ California State University, Department of Physics, Fullerton, CA 92634, USA
‖ Electronic Structure of Materials Centre, The Flinders University of South Australia, GPO Box 2100, Adelaide 5001, Australia
¶ University of California, Los Alamos National Laboratory, Los Alamos, NM 87544, USA

Received 6 January 1998, in final form 3 March 1998

Abstract. The results of a combined experimental and theoretical study of elastic electron scattering by laser-excited ^{138}Ba$(\ldots 6s6p\ ^1P_1)$ atoms are presented. From these studies, we extracted differential scattering cross sections and parameters for elastic scattering both by coherently prepared $^1P_1$ Ba atoms and by Ba atoms in an isotropic, incoherent state of the $^1P_1$ level. This is the first time that results of this type have been reported for elastic scattering by excited atoms. Good agreement was found between the limited experimental results and those obtained from our convergent close-coupling (CCC) theoretical calculations. It was demonstrated that elastic scattering can create alignment with significant probability.

Previous electron scattering studies of laser-excited atoms have been restricted primarily to superelastic scattering and to the interpretation of these experiments in terms of electron-impact coherence parameters (EICPs) for the 'inverse', inelastic, collision process (see e.g. Hertel and Stoll 1974a, b, Zetner *et al* 1990, Li and Zetner 1994, Hall *et al* 1996, Teubner *et al* 1996 and references therein). These parameters characterize the atomic state prepared by the electron collision process and allow us a deeper insight into the nature of this process than conventional differential cross section measurements permit. To date, no experiments of this type have been reported on *elastic* electron scattering by coherently excited atoms. However, experimental data of this type are needed for gaining insight into the dynamics of electron scattering by excited atoms to test recently developed calculational methods and to answer the question raised in connection with plasma polarization spectroscopy as to whether elastic electron scattering can create alignment and to what degree (see Petrashen *et al* 1984, Dashevskaya and Nikitin 1987).

We describe here measurements of *elastic* electron scattering by ^{138}Ba$(\ldots 6s6p\ ^1P_1)$ atoms which were coherently prepared by a linearly polarized laser beam. These measurements allowed us to extract various differential cross sections, EICPs and collision parameters for elastic scattering. In a parallel theoretical effort, we used the convergent-close-coupling (CCC) approximation, along with the LS-coupling scheme, to calculate all

+ Present address: MPB Technologies, Pointe Claire, Quebec H9R 1E9, Canada.

0953-4075/98/080393+08$19.50

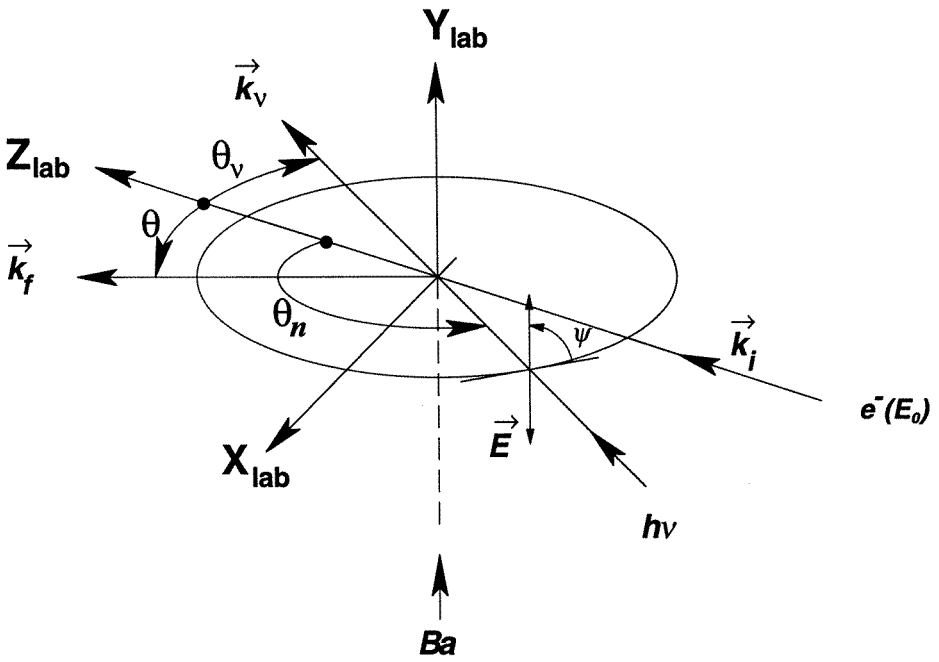

Figure 1. Schematic experimental arrangement. The laboratory coordinate system is shown and the directions of the three beams are indicated.

the cross sections and parameters derived from the experiments. Measurements were carried out at an electron impact energy (E_0) of 20.0 eV and scattering angles (θ) of $10^\circ, 15^\circ$ and 20°. Calculations were performed at $E_0 = 2.8, 20.0$ and 97.8 eV over the entire 0°–180° angular range in 1° steps.

The experimental arrangement is shown schematically in figure 1 and has been described previously (Zetner *et al* 1990). A collimated atomic Ba (naturally occurring isotopic mixture) beam was crossed at 90° by a nearly monoenergetic ($\Delta E_{1/2} \approx 0.08$ eV) electron beam. The interaction region was illuminated by a linearly polarized laser beam which was located in the scattering plane and was produced from a ring laser, operating in single mode. The laser wavelength was tuned to excite the $^{138}\mathrm{Ba}\left(\ldots 6s^2\ {}^1\mathrm{S}_0 \rightarrow \ldots 6s6p\ {}^1\mathrm{P}_1\right)$ transition. The elastic scattering signal was measured at a fixed (E_0, θ) for fixed laser geometries with respect to the laboratory frame (θ_ν, ϕ_ν) as a function of the linear polarization angle (ψ) width respect to the scattering plane.

The measured count rates (I_{TOT}) in the elastic scattering experiment include contributions from background (I_{B}), from elastic scattering by ground state atoms of all isotopes ($I_{\mathrm{G}}^{\mathrm{el}}$), and from elastic scattering by coherently excited $^1\mathrm{P}_1$ ($I_{\mathrm{cP}}^{\mathrm{el}}$) and cascade populated $^3\mathrm{D}_2$ and $^1\mathrm{D}_2$, metastable ($I_{\mathrm{m}}^{\mathrm{el}}$) ^{138}Ba atoms. In order to assure identical experimental conditions for the modulation measurements, to separate $I_{\mathrm{cP}}^{\mathrm{el}}$ from other contributions to the measured signal and to obtain absolute cross sections and parameters from the experiments, we needed to carry out 116 measurements of various kinds for each fixed (E_0, θ) case. These measurements involved the inelastic $\left({}^1\mathrm{S}_0 \rightarrow {}^1\mathrm{P}_1\right)$, the superelastic $\left({}^1\mathrm{P}_1 \rightarrow {}^1\mathrm{S}_0\right)$ and the elastic scattering channels. Scattering intensities for various combinations of the Ba beam and laser beam turned on and off, at two laser positions (laser in the scattering plane and laser displaced by about 4 mm parallel to the scattering plane upstream of the Ba beam) and

for four laser geometries ($\theta_v = 45^\circ$ and 90°, both with $\phi_v = 0^\circ$ and 180°) were measured and the modulation of the elastic and superelastic scattering intensities as a function of ψ was determined. Normalization of the $I^{\rm el}_{\rm cP}(\psi)$ signal to the corresponding differential cross section, $\mathrm{DCS}^{\rm el}_{\rm cP}(\psi)$, was achieved by measuring the ratio of this elastic scattering signal to the signal associated with $\left({}^1\mathrm{S}_0 \rightarrow {}^1\mathrm{P}_0\right)$ inelastic scattering and utilizing the derived population fractions and the $\left({}^1\mathrm{S}_0 \rightarrow {}^1\mathrm{P}_0\right)$ inelastic differential cross section values of Wang *et al* (1994).

At this stage, we have (for a fixed (E_0, θ) case) a modulation equation of the type

$$\mathrm{DCS}^{\rm el}_{\rm cP}(\psi) = \tfrac{3}{4}\mathrm{DCS}^{\rm el}_{\rm P}\{A + B\cos 2\psi\} \tag{1}$$

for each laser geometry (Zetner *et al* 1990). The values of A and B were obtained from least-squares fitting of the experimental data. They contain factors related to the laser geometry and parameters related to the physics of the electron–atom collision. Measurements with several laser geometries are needed to obtain these parameters. We denote here the differential cross sections associated with scattering processes where the initial atomic states are prepared by coherent excitation to the ${}^1\mathrm{P}_1$ state with a particular laser geometry and polarization as $\mathrm{DCS}^{\rm el}_{\rm cP}(\psi)$. For differential cross sections associated with processes where the initial and/or final magnetic sublevel is specified (or averaged-over incoherently), we use the notation $\mathrm{DCS}^{\rm el}_{\rm P}(M_i, M_f)$, $\mathrm{DCS}^{\rm el}_{\rm P}(M_i = M)$, $\mathrm{DCS}^{\rm el}_{\rm P}(M_f = M)$ and $\mathrm{DCS}^{\rm el}_{\rm P}$. Omission of M_i and/or M_f implies averaging (summation) over those magnetic sublevel quantum numbers. M can take the values of $-1, 0$ or $+1$. (We select for the quantization axis for the magnetic sublevel cross sections the incoming electron momentum vector.) Since the spin of the scattering electrons was not selected or detected in the present measurements, averaging over initial and summation over final spin quantum numbers are always assumed.

The modulation equation (1) can be used in two different ways: (i) to obtain EICPs and differential cross sections for the hypothetical 'inverse' process, i.e. for elastic scattering by an isotropic, incoherent state of ${}^{138}\mathrm{Ba}\left(\ldots 6\mathrm{s}6\mathrm{p}\ {}^1\mathrm{P}_1\right)$ atoms and (ii) to obtain collision parameters and differential cross sections for elastic scattering by the coherently prepared ${}^{138}\mathrm{Ba}\left(\ldots 6\mathrm{s}6\mathrm{p}\ {}^1\mathrm{P}_1\right)$ atoms.

For evaluation of the modulation equations in terms of the hypothetical 'inverse' process (based on the theory of Macek and Hertel (1974)), we have for the modulation coefficients (Zetner *et al* 1990):

$$A = 1 + \cos^2\theta_n + \lambda\left(1 - 3\cos^2\theta_n\right) + (\lambda - 1)\cos\varepsilon\sin^2\theta_n + \kappa\sin 2\theta_n\cos\phi_n \tag{2a}$$

$$B = (3\lambda - 1)\sin^2\theta_n + (1 - \lambda)\cos\varepsilon\left(1 + \cos^2\theta_n\right) + \kappa\sin 2\theta_n\cos\phi_n \tag{2b}$$

where

$$\kappa = 2\sqrt{\lambda(1-\lambda)}\cos\chi = 2\sqrt{\lambda(1-\lambda)}\cos\Delta\cos\tilde{\chi}. \tag{2c}$$

In the present experiments, $\theta_n = \theta_v + \theta\cos\phi_n$ and for scattering to the left we have $\phi_v = 180^\circ$ and $\phi_n = \phi_v - \pi = 0^\circ$ and for scattering to the right we have $\phi_n = \phi_v = 180^\circ$. The modulation equations involve the four EICPs ($\lambda, \cos\varepsilon, \cos\Delta$ and $\tilde{\chi}$) as defined by da Paixão *et al* (1980) and applied to the Ba superelastic scattering by Zetner *et al* (1990). From our laser-in-plane measurements we can extract only $\lambda, \cos\varepsilon$ and κ. These EICPs can be obtained by solving any set of three equations defining A or B for laser geometries with $\theta_v = 45^\circ$ and 90°. There are 16 meaningful such combinations, each yielding a set of EICPs. We took the average of these 16 sets as our experimental values. Definition of these EICPs and their relations to various cross sections and scattering amplitudes for a $\left({}^1\mathrm{S}_0 \leftrightarrow {}^1\mathrm{P}_1\right)$ process is given by Zetner *et al* (1990). The only difference here is the generalization from the $\left({}^1\mathrm{S}_0 \leftrightarrow {}^1\mathrm{P}_1\right)$ to the $\left({}^1\mathrm{P}_1 \leftrightarrow {}^1\mathrm{P}_1\right)$ transition, which requires averaging over the initial

magnetic sublevels of the $^1P_1$ level. From λ and DCS_P^{el}, we obtained $DCS_P^{el}(M_f = 0)$. From $DCS_P^{el}(M_f = 0)$ and DCS_P^{el}, the $DCS^{el}(M_f = 1)$ values were calculated. DCS_P^{el} was obtained by taking the average of $DCS_{cP}^{el}(\psi_m)^+$ and $DCS_{cP}^{el}(\psi_m)^-$ where ψ_m is the polarization angle satisfying the condition $\cos 2\psi_m = \frac{1}{3}$ and the superscript $+(-)$ refers to $\phi_v = 0^\circ$ (180°).

For the evaluation of the modulation equations in terms of the actual experimental (forward) process (as described above under (ii)), we used equations of the same form as (2*a*)–(2*c*), except $\lambda, \cos\varepsilon, \kappa, \cos\Delta$ and $\cos\tilde{\chi}$ were replaced by p_1, p_2, h, p_3 and p_4, respectively, and $\theta_n = \pi - \theta_v$. These equations are formally similar to equations (2*a*)–(2*c*) and can be derived in a straightforward manner (Li and Zetner 1996, Zetner 1997). The collision parameters, p_1, p_2 and h were obtained from a procedure similar to that described above for the EICPs. These parameters are useful, in the sense that they allow us to calculate the $DCS_{cP}^{el}(\psi)$ value associated with *any initial state* prepared by in-plane laser excitation of arbitrary geometry and linear polarization.

The CCC calculations performed for electron scattering by ground state light atoms (Li, Karaganov *et al* 1996; Na, Bray 1994; He, Fursa and Bray 1995) showed excellent agreement with experimental results. It is therefore of interest to the atomic physics community to check the applicability of this method to heavier elements like Ba and to atoms not in their ground states. The present e^-–Ba scattering calculations have been performed by using the CCC method in the non-relativistic LS-coupling framework (see Fursa and Bray 1997 for details). In brief, the barium atom was considered to have two active valence electrons above an inert Hartree–Fock core. Phenomenological one- and two-electron polarization potentials have been added to account for the core polarization. Configuration–interaction (CI) expansions have been used to obtain the Ba wavefunctions. One-electron orbitals have been obtained from the diagonalization of the Ba^+ Hamiltonian in the Sturmian (Laguerre) basis. This allowed us to obtain a good description of the barium discrete states and to achieve square-integrable discretization of the Ba continuum. All negative-energy states (relative to the Ba^+ ground state) and a large number of positive energy states (representing coupling to the ionization continuum) have been included in the CCC calculations. The total number of states used in the present calculations was 115. They consisted of 14 ^1S, 17 $^1P^o$, 19 $^1D^o$, 19 $^1F^o$, 7 ^3S, 9 $^3P^o$, 9 $^3D^o$, 9 $^3F^o$ and two each of $^{1,3}P^o$, $^{1,3}D^o$ and $^{1,3}F^o$ states.

Selected values of the large set of the measured and calculated cross sections and parameters are shown in figures 2 and 3, respectively. The estimated experimental error limits for these quantities are 30% for the differential cross sections and λ and p_1 parameters and 40% for the $\cos\varepsilon$ and p_2 parameters. The h and k parameters extracted from the present measurements are found to be unreliable. This is due to the fact that these parameters are small compared to the errors associated with the modulation coefficients and to the nature of error propagation. A reliable extraction of these parameters would require the knowledge of the modulation coefficients to within an accuracy of about 1%.

In figure 2, three theoretical differential cross sections are shown over the full angular range and compared to the experimental results. The experimental and theoretical results agree well within the estimated experimental error limits. The values for these cross sections drop by almost five orders of magnitude between 0° and 70°. It is clear from the present study that the cross sections at high scattering angles are very small and their measurement would be extremely difficult. Therefore, one will have to rely on the theoretical calculations in these regions. A 'shoulder' with an inflection point at around 35° and two deep minima at around 72° and 134° appears in the theoretical curves. The same general behaviour is found for the other $DCS_P^{el}(M_i = M)$ and $DCS_P^{el}(M_f = M)$ curves. They not only show

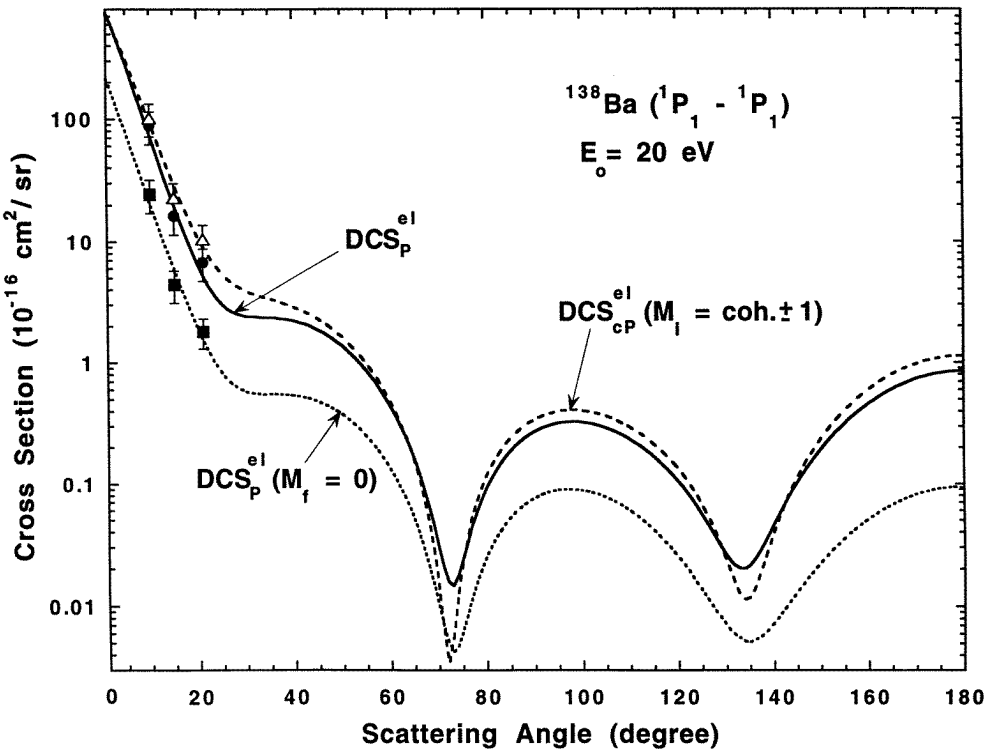

Figure 2. Elastic differential electron scattering cross sections for $^{138}\mathrm{Ba}(^1\mathrm{P}_1)$ atoms at $E_0 = 20$ eV. Curves represent the results of CCC calculations. The corresponding experimental values are indicated by symbols. Experimental error limits are also shown.

the same general shape but also have the same order of magnitude values (except the $\mathrm{DCS}_\mathrm{P}^{\mathrm{el}}(M_f = M)$ curves are multiplied by the factor of $1/(2J_i + 1) = \frac{1}{3}$ coming from the averaging over M_i). The $\mathrm{DCS}_{\mathrm{cP}}^{\mathrm{el}}(M_i = \mathrm{coh}\pm 1)$ curve shows deeper and sharper minima than the others ($M_i = \mathrm{coh}\pm 1$ refers to an initial state which is a coherent superposition of the $+1$ and -1 magnetic sublevels with equal coefficients). The reason for this similarity is that the dominant terms (corresponding to $\Delta M = 0$) in the averaging are similar in all cases. These observations indicate no strong dependence on M_i and M_f for $\mathrm{DCS}_\mathrm{P}^{\mathrm{el}}(M_i = M)$ and $\mathrm{DCS}_\mathrm{P}^{\mathrm{el}}(M_f = M)$, respectively. The calculations show that the various $\mathrm{DCS}_\mathrm{P}^{\mathrm{el}}(M_i, M_f)$ values differ by more than an order of magnitude but these differences are eliminated, to a large extent, in the averaging processes. The difference in $\mathrm{DCS}_\mathrm{P}^{\mathrm{el}}(M_f = 1)$ and $\mathrm{DCS}_\mathrm{P}^{\mathrm{el}}(M_f = 0)$ values, which determines the alignment creation cross section, is, however, significant at most scattering angles.

In figure 3 the EICPs, λ and $\cos\varepsilon$ are shown. Not surprisingly, very good agreement between experiment and theory is found for λ, since it represents the ratio of two cross sections which both show, separately, good agreement between experiment and theory. Somewhat less satisfactory is the agreement for $\cos\varepsilon$. While no significant features appear in the λ curve, the $\cos\varepsilon$ curve shows a deep minimum at around 22° and two sharp maxima at around 72° and 135°. These maxima are associated with the deep minima in the $\mathrm{DCS}_{\mathrm{cP}}^{\mathrm{el}}(M_f = 1)$ which appear as the denominator in the definition of $\cos\varepsilon$. The deviation of $\cos\varepsilon$ from the value of unity for the theoretical curve is strictly due to the averaging

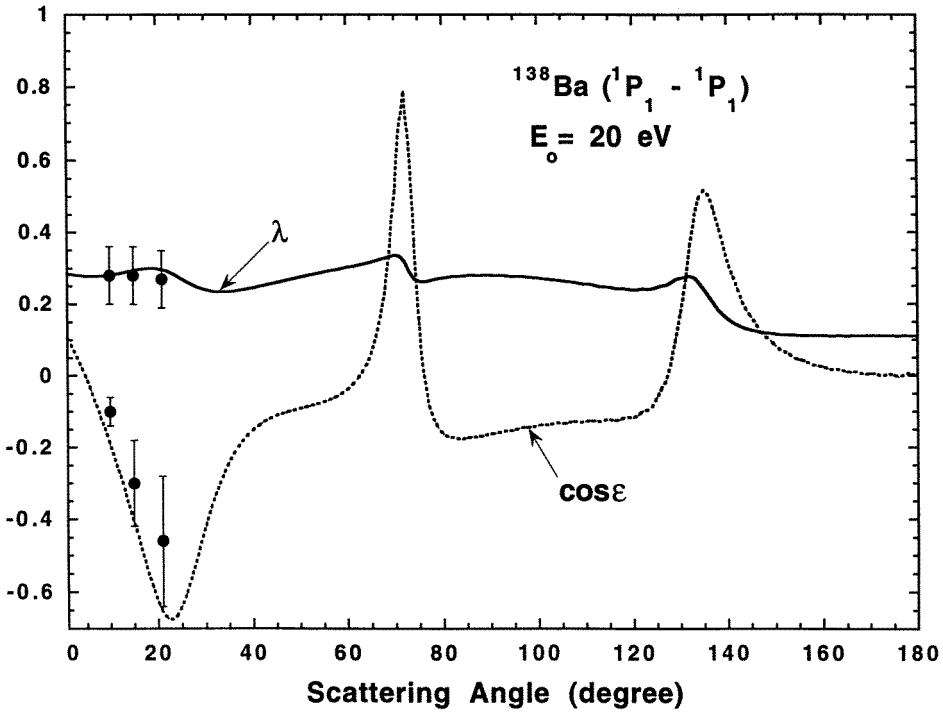

Figure 3. The EICPs (λ and $\cos\varepsilon$) for elastic electron scattering by $^{138}\mathrm{Ba}(^1\mathrm{P}_1)$ atoms at $E_0 = 20$ eV. ● indicates the present experimental results with error limits, the curves are from the present CCC calculations.

over M_i which causes the loss of coherence between the $M_f = 1$ and $M_f = -1$ scattering amplitudes. For the experimental value, some loss of coherence may also be due to spin–orbit coupling effects and this may account to some extent for the less satisfactory agreement between experiment and theory.

The angular behaviours of the collision parameters p_1 and p_2 are very similar to those of λ and $\cos\varepsilon$, respectively. The agreement between theory and experiment can also be similarly characterized. It should be noted that the EICPs ($\lambda, \cos\varepsilon, \cos\Delta$ and $\tilde{\chi}$) are related to the collision parameters (p_1, p_2, p_3 and p_4) by transformation of the scattering amplitudes involved from the inverse to the forward reference frame. These reference frames are constructed so that the Z-axes correspond to the momentum vectors of the incoming electrons, the X-axes taken to be on the same side of the Z-axes as the momentum vector for the outgoing electron and the Y-axes to form right-handed coordinate systems (see e.g. Bartschat 1989).

Considering the complexity of the experiments and the fact that the theoretical calculations neglect spin–orbit coupling effects, the general agreement between theory and experiment is surprisingly good for the $E_0 = 20$ eV, $\theta = 10^\circ, 15^\circ, 20^\circ$ cases. This agreement indicates that extended scattering volume effects (see Zetner *et al* 1990) are not important in the present measurements and that the CCC calculational scheme, used here, is applicable to elastic scattering by $\mathrm{Ba}(^1\mathrm{P}_1)$ atoms. The rate of convergence and the importance of the ionization channels in our calculations were investigated by also performing calculations with 55 discrete states in the expansion. The results of these calculations were found to be in reasonably good agreement with those described here

Table 1. Integral cross sections for elastic electron scattering by $^{138}\mathrm{Ba}(\ldots 6s6p\ ^1\mathrm{P}_1)$ atoms (in 10^{-16} cm^2 units). $Q(^1\mathrm{S}_0 \leftrightarrow {}^1\mathrm{S}_0)$ at $E_0 = 20$ eV: experiment (Wang *et al* 1994), 26.7; CCC calculation (Fursa and Bray 1997), 29.4.

	2.8 eV	20.0 eV	97.8 eV
$Q(1,1) = Q(-1,-1)$	119.7	36.6	18.1
$Q(1,0) = Q(-1,0)$	2.0	0.74	0.054
$Q(1,-1)$	4.6	1.6	0.37
$Q(0,0)$	89.3	28.5	14.7
$Q(0,-1) = Q(0,1)$	1.2	0.62	0.054
$Q(M_f = 0)$	31.1	10.0	4.9
$Q(M_f = 1) = Q(M_f = -1)$	41.8	12.9	6.2
$Q(M_i = 0)$	91.6	29.8	14.8
$Q(M_i = 1) = Q(M_i = -1)$	126.3	39.0	18.5
Q	114.7	35.9	17.3
$Q_{\mathrm{CR}}^{[2]}$	8.7	2.4	1.0

(which included 115 states and accounted for coupling to the target ionization continuum). The reason for this agreement is that the dipole polarizability for the $\mathrm{Ba}(6s6p\ ^1\mathrm{P}_1)$ state is dominated by the discrete spectrum. The neglect of spin–orbit coupling in our calculations is justified by the good agreement between experiment and theory. The major effect of spin–orbit coupling in our case manifests itself in singlet–triplet mixing for the target atom. It is well known, however, that the mixing coefficient for the $^3\mathrm{P}_1$ LS term is small (see e.g. Bauschlicher *et al* 1985).

With the assurance given by the good agreement between experiment and theory, we extended the CCC calculations to other scattering angles and impact energies to obtain the various integral elastic scattering and the alignment creation $\left\{Q_{\mathrm{CR}}^{[2]} = \left(\frac{2}{3}\right)^{1/2}[Q(M_f = 1) - Q(M_f = 0)]\right\}$ cross sections. Some of these cross sections are listed in table 1, which also shows for the purpose of comparison experimental and calculated integral elastic scattering cross sections for ground state Ba atoms at $E_0 = 20$ eV. This table shows that alignment can be created by elastic scattering and gives us some indication concerning the magnitude of the alignment creation cross section.

Details of the experiments and calculations will be presented in a future publication.

The authors acknowledge financial support by NSF, NASA, NRC and DOE. Support of the South Australian Centre for High Performance Computing and Communications is also acknowledged. We wish to express our gratitude to T Fujimoto and S A Kazantsev for calling our attention to the question of alignment creation in elastic scattering and for valuable discussions. We also acknowledge important communications with P W Zetner and D C Cartwright.

References

Bartschat K 1989 *Phys. Rep.* **180** 1
Bauschlicher C W Jr, Jaffe R L, Langhoff S R, Mascarello F G and Partridge H 1985 *J. Phys. B: At. Mol. Phys.* **18** 2147
Bray I 1994 *Phys. Rev.* A **49** 1066
Dashevskaya E I and Nikitin E E 1987 *Sov. J. Chem. Phys.* **4** 1934
da Paixão F J, Padial N T, Csanak G and Blum K 1980 *Phys. Rev. Lett.* **45** 1164

Fursa D V and Bray I 1995 *Phys. Rev.* A **52** 1279
——1998 to be published
Hall B V, Sang R T, Shurgalin M, Farrell P M, MacGillivray W R and Standage M C 1996 *Can. J. Phys.* **74** 977
Hertel I V and Stoll W 1994a *J. Phys. B: At. Mol. Opt. Phys.* **7** 570
——1994b *J. Phys. B: At. Mol. Opt. Phys.* **7** 583
Karaganov V, Bray I, Teubner P J O and Farrell P 1996 *Phys. Rev.* A **54** R9
Li Y and Zetner P W 1994 *J. Phys. B: At. Mol. Opt. Phys.* **27** L293
——1996 *J. Phys. B: At. Mol. Opt. Phys.* **29** 1803
Macek J and Hertel I V 1974 *J. Phys. B: At. Mol. Phys.* **7** 2173
Petrashen A G, Rebane V N and Rebane T K 1984 *Opt. Spectrosc. (USSR)* **55** 492
Teubner P J O, Karaganov V, Law M R and Farrell P M 1996 *Can. J. Phys.* **74** 984
Wang S, Trajmar S and Zetner P W 1994 *J. Phys. B: At. Mol. Opt. Phys.* **27** 1613
Zetner P W 1997 Private communication
Zetner P W, Trajmar S and Csanak G 1990 *Phys. Rev.* A **41** 5980